Optica Applicata, Vol. XXXI, No. 3, 2001

Spectral phenomena in CO_2 lasers. A review

EDWARD F. PLIŃSKI

Wrocław University of Technology, Institute of Telecommunications and Acoustics, Wybrzeże Wyspiańskiego 27, 50–370 Wrocław, Poland.

A rich spectrum of the CO_2 molecule is an appreciated advantage of lasers based on the carbon dioxide medium. On the other hand, that specific feature of the CO_2 molecule brings about many problems. Sometimes it can be a serious obstacle in designing laser devices. The paper gives an overview of the spectral properties of the radiation of different kinds of CO_2 lasers. Many examples of the spectral phenomena are presented on modern RF excited waveguide, multi-waveguide and slab-waveguide CO_2 lasers.

1. Introduction

The present paper focuses on spectral contents of the laser output beam, mode structures, line profiles or free spectral ranges. Spectral properties of the laser radiation, as a subject under consideration, include such spectral phenomena as a Lamb dip, inverted Lamb dip, an absorption peak. In other words, the subject covers everything that is connected with a laser frequency and an emission line. Spectral phenomena appearing in CO_2 lasers are mostly neglected in designing CO_2 technological lasers. Indeed, most of the laser technological devices are not sensitive to fine changes of the laser radiation wavelength. But some applications need a good knowledge about specific, spectral features of the molecular CO_2 lasers, which distinguish them from much simpler gas atomic lasers. One of the examples is heterodyning technique applied in heterodyne spectroscopy [1], or in measurements of absolute frequency of the CO_2 hot bands [2]. It is often used where the intermediate frequency between known and unknown oscillators is too big for direct measurements. It can be used as a very sensitive detector of the spectral contents of the output radiation in both continuous wave and pulse regimes. A simplified technique, known as a homodyne one, is a very useful tool for measurements of intermode beats in the range of the laser emission line width, that is, for investigation of the spectral contents of the output laser beam, like "hooting" modes [3]. A very specific phenomenon for CO_2 lasers, which is a laser signature, can be used as a diffractive scanning mechanism for laser markers [4]. But independent signatures of each laser channel of the CO_2 laser arrays impose limitations on the quality of the total laser beam [5], [6]. Knowledge about the signature created over the pulse duration of the CO_2 lasers in pulse regime can be very useful for estimation of the refractive index changes of the laser medium. It involves knowledge of the dynamic behaviour of pressure and temperature in the laser cavity [7]. Because

of the long wavelength emitted, the CO_2 laser can penetrate molecular spectra and, as a consequence, it can be applied to optical pumping of the FIR laser media [8], [9]. Different techniques of the CO_2 laser spectrum spreading like a technique of sequence bands [10]–[12], or electronic-to-vibrational energy transfer from an excited Br_2 molecule to a CO_2 molecule [13], or isotope shift technique [14]–[17] also belong to the subject matter considered here. A pulling effect, blue and red shifts [18], [19] are other spectral phenomena important in stabilisation of the frequency of the laser radiation. On the other hand, sophisticated stabilisation techniques are based on such phenomena as a Lamb dip [20]–[23], an inverted Lamb dip or an absorption peak [24], [25]. These techniques are used in a laser saturated spectroscopy [26]–[28]. The technique applied to frequency stabilisation of CO_2 lasers requires a very detailed knowledge about a CO_2 spectrum and molecules used in a saturation absorption method of the laser stabilisation, *e.g.*, stabilisation to the centre of the SF_6 absorption peak [29] or to the centre of the OsO_4 absorption peak [30]. Another stabilisation technique, 4.3 μm saturation resonance is also based on spectral properties of the CO_2 molecule used as an internal absorber in the laser cavity [31]. Continuing the subject, it should be mentioned that the CO_2 laser was used in communication experiments at 10.6 μm transmitting successfully a television picture [32]. The CO_2 laser spectral range can also be used in laser radars and lidars [33].

Understanding of the CO_2 laser spectral properties and knowledge about spectral phenomena appearing in CO_2 lasers can help in designing the laser devices.

2. Spectrum of the CO_2 molecule

Spectroscopy of the CO_2 molecule is described by a system of energy levels typical for symmetrical molecules. Figure 1 shows a well-known simplified diagram of the CO_2 energy levels (mainly vibration levels spread into rotational ones) important for the laser action. The vibrational levels, taking part in the laser action, are close to the ground 00^00 state and the distances between them are relatively small. As a consequence, transitions between levels belong to the infrared region (9–12 μm). The CO_2 molecule can oscillate in three vibration modes: symmetric, bending and asymmetric. It forms three groups of energy levels: $n00$, $0n0$ and $00n$, respectively, where $n = 0, 1, 2, \ldots$. The laser transitions can proceed between rotational states of neighbouring oscillation levels. Figure 2 shows the distribution of population of the selected vibrational line. The population n_{vj} (v – vibrational number, j – rotational number) of the level is expressed by [34]:

$$n_{vj} = N_v \left(\frac{2hcB_v}{kT}\right)(2j+1)\exp\left\{-\frac{hc}{kT}\left[B_v j(j+1) - D_v j^2(j+1)^2\right]\right\} \tag{1}$$

where: N_v – total population of level v, h – Planck constant, c – speed of light, k – Boltzmann constant, T – temperature, B_v and D_v – rotational constants.

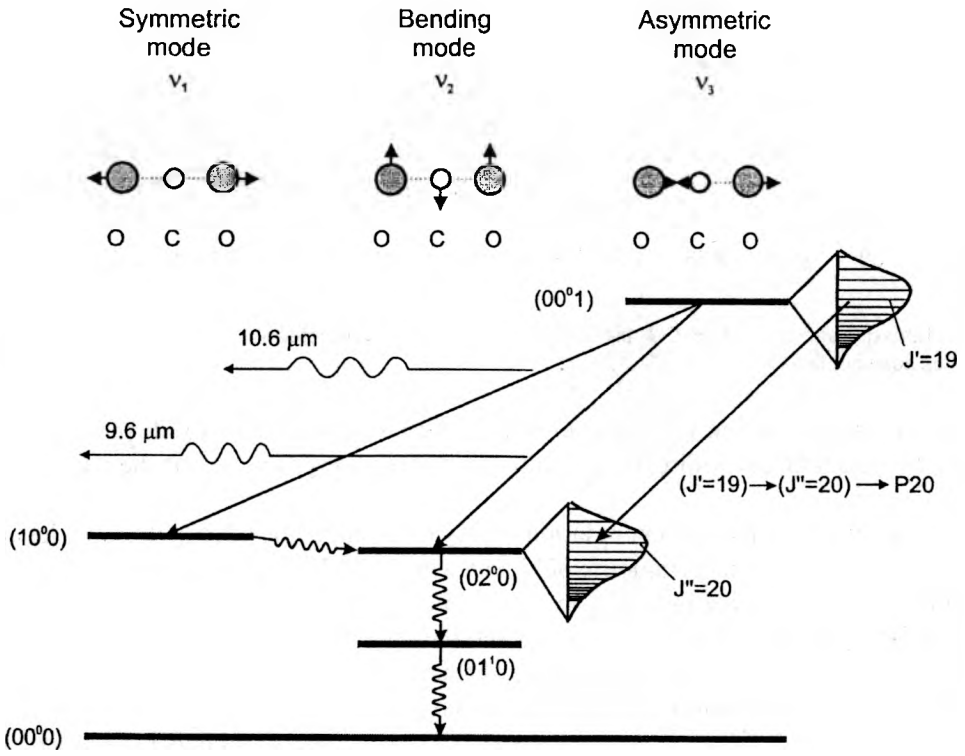

Fig. 1. Simplified system of energy levels of a CO_2 molecule (N_2 molecule is not indicated).

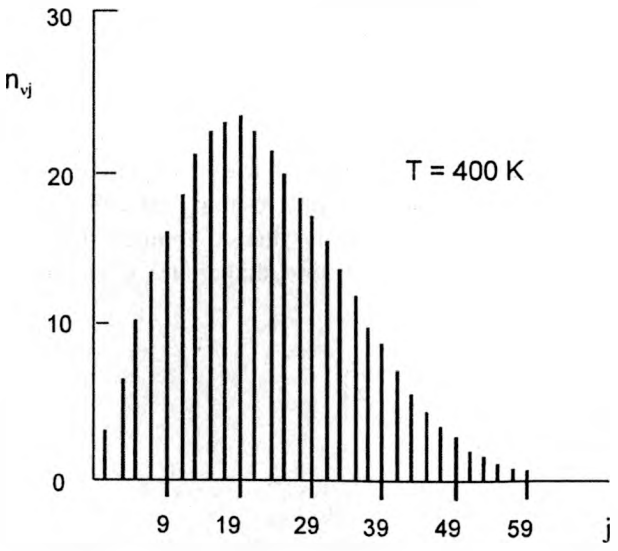

Fig. 2. Population n_{vj} of the rotational levels j of CO_2 molecule.

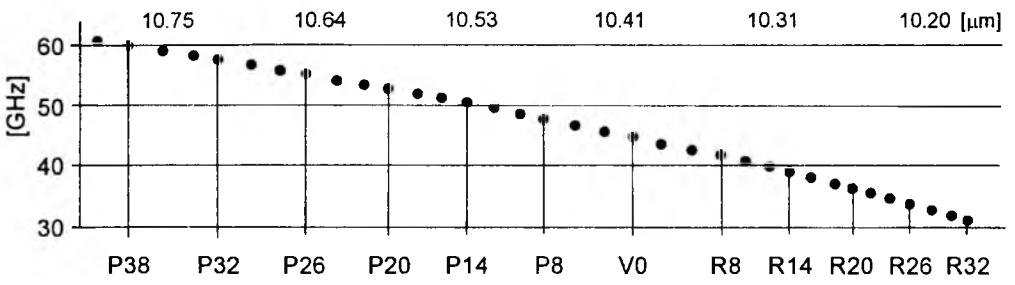

Fig. 3. Emission spectrum of the CO_2 laser – the 10.4 μm band – presented as the distances in frequency between adjacent lines.

The existence of that kind of energy level structure results in a rich spectrum of the CO_2 molecule and it directly determines the spectral properties of the CO_2 laser radiation.

The inversion of the level population is easy to obtain at the 00^01 metastable level. The transitions between asymmetric 00^01 and symmetric 10^01 or asymmetric 00^01 and bending 02^00 levels give radiation in the medium infrared region at wavelengths of around 10.4 μm or 9.4 μm, commonly called the regular bands of the CO_2 spectrum. Figure 3 shows the 10.4 μm band of the CO_2 laser spectrum. (Traditionally that band is called the 10.6 μm because of the strongest laser radiation at that wavelength). Two branches can be distinguished in the band: *P* and *R*. The *P* branch is created for transitions of type $j(00^01) - j(10^01) = -1$, the *R* branch is created for transitions of type $j(00^01) - j(10^01) = 1$. The distance in frequency between two adjacent emission lines changes for the 10.4 μm band from about 30 to 60 GHz. This picture is worth emphasizing because such laser inter-frequencies are applied as a source in heterodyne spectroscopy of signals coming from the space.

3. Shape of the CO_2 gain line

The emission (or absorption) line width, so called a natural width, depends on the lifetime of the energy levels, and it is usually broadened due to many factors such as collisions and heterogeneity of the medium, but mainly due to temperature and pressure. A pressure broadened, or Doppler broadened, line shape $S(\nu, \nu_{12})$ can be described by the expression

$$S(\nu, \nu_{12}) = \frac{c}{\nu_{12}}\left(\frac{M}{2\pi kT}\right)^{1/2} \exp\left[-\frac{Mc^2}{2kT\nu_{12}^2}(\nu - \nu_{12})^2\right] \tag{2}$$

where M – mass of the molecule.

The frequency of transition ν_{12} is translated into the frequency $\nu = \nu_{12} - (1 + \nu_x/c)$, where ν_x – velocity of the molecule in observation direction x.

Analysing one chosen spectral line for typical CO_2:N_2:He laser mixture as a function of pressure we can distinguish two characteristic shapes of the line. The first one is an inhomogeneously Doppler broadened line with Gaussian shape (up to approximately 1 Tr). For low pressures the Doppler width $\Delta\nu_D$ of the line is given by the formula

$$\Delta\nu_D = 2\nu_0\sqrt{\frac{2kT}{Mc^2}\ln 2} \tag{3}$$

where ν_0 – central frequency of the line.

For temperature of $T \approx 550$ K the Doppler width equals approximately 60 MHz. Above the pressure of 1 Tr we have a homogeneously broadened Lorentzian shape. All kinds of CO_2 lasers operate at much higher pressures in a homogeneous region (dc, TEA, RF excited, waveguide, gas-dynamic lasers). The broadening of the gain line is given by the formula [34]

$$\Delta\nu_p = 7.58(\psi_{CO_2} + 0.73\psi_{N_2} + 0.64\psi_{He})p\sqrt{\frac{300}{T}} \quad \text{[MHz]} \tag{4}$$

where: ψ_x – fraction of the x component, p – total pressure.

It is interesting to consider very high pressure CO_2 lasers (above 10 atm). In that case the pressure broadening is comparable to the CO_2 line distances (see Fig. 3), and spectral lines overlap them self-creating a continuous band.

4. Heterodyne and homodyne technique

The heterodyning is one of the most sensitive measuring techniques. The method enables very high frequencies inaccessible for frequency meters to be measured in an indirect way. The method consists in measuring the intermediate frequency between two frequency sources: the known one as a reference, and unknown one. Sometimes more independent frequency sources connected in a chain are necessary to measure the absolute frequency of some oscillators. They are usually used where the intermediate frequency between known and unknown oscillators is too big for the direct measurement. Sometimes, to see the spectral contents of the laser output beam it is enough to use the homodyne detection where the single-mode source laser is not necessary.

4.1. Heterodyne spectroscopy

One of the applications of the heterodyne measurements is heterodyne spectroscopy. The method is used in astronomy and investigations of the distributions of the trace gases (CO, NH_3, O_3) in Earth's atmosphere. It covers the wavelength range from 30 μm to 1 mm. The method is based on the "superheterodyne" technique that is well known in radiocommunication. The purpose of the superheterodyne receiver is to translate a signal from one frequency to another. It is particularly suitable when direct

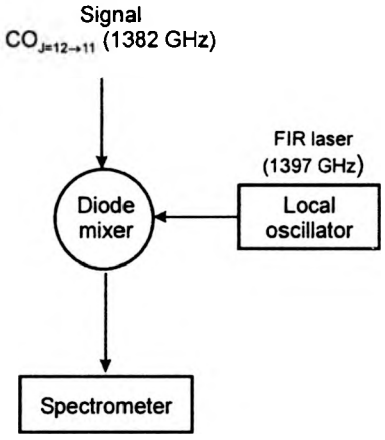

Fig. 4. Schematic block diagram for a heterodyne spectrometer [1]. The intermediate frequency is approx. 15 GHz between measured carbon monoxide radiation and FIR laser as a reference source.

T a b l e 1. Local oscillator lines for the detection of CO [1].

FIR laser molecule	Wavelength [μm]	Frequency [GHz]	Pumping line CO_2 laser	CO molecule transitions	Frequency [GHz]	Intermadiate frequency [GHz]
HCOOH	432.6	962.9514	9.6 R20	$J = 6–5$	691.5	1.4
$^{15}NH_3$	373.4	802.9870	10.6 R42	$J = 7–6$	806.7	3.7
CH_2F_2	289.4	1035.5527	9.6 P4	$J = 9–8$	1036.9	1.3
CH_2F_2	287.7	1042.1504	9.6 R34	$J = 9–8$	1036.9	5.2
CH_2F_2	235.7	1272.1714	9.6 R34	$J = 11–10$	1267.0	5.2
CH_2F_2	214.5	1397.1186	9.6 R34	$J = 12–11$	1381.9	15.1
CH_2F_2	184.3	1626.6026	9.6 R32	$J = 14–13$	1611.8	14.8
CH_3OH	163.0	1838.8393	10.6 R38	$J = 16–15$	1841.3	2.5
CH_3OH	118.8	2522.7816	9.6 P36	$J = 22–21$	2528.2	5.4

detection of the signal is impossible like in the case of the range from 200 μm to 500 μm. Figure 4 shows the heterodyne spectrometer used for detection of CO in Earth's atmosphere. The incoming high frequency signal is mixed in non-linear resistance of the detector with a local oscillator beam. The frequency of the oscillator is close to the signal frequency. In this way, the high frequency signal under investigation is translated down to the microwave range and there is not any

information lost. The main element of the FIR laser is a carbon dioxide laser that is used as a pumping source for the submillimetre medium. Table 1 shows some FIR laser oscillator lines for the detection of carbon monoxide and pumping CO_2 lines.

4.2. Heterodyne frequency measurements of CO_2 sequence band lines

The absolute frequency of the sequence CO_2 laser lines can be measured by heterodyning with well known CO_2 laser regular frequencies of the 00^01–$(10^00, 02^00)$ bands. Figure 5 shows the setup for heterodyne measurements of the absolute frequencies of the sequence bands [2]. (The system measures the intermediate frequencies between known – regular and unknown – sequence lines). The sequence

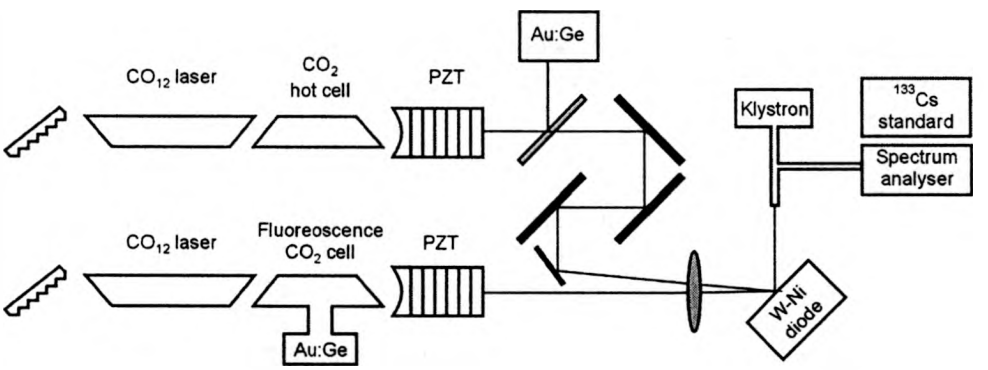

Fig. 5. Setup for measurements of the beat frequencies between the sequence ν_s and regular ν_r lines of the CO_2 laser. Explanation in the main text.

Table 2. 00^02–10^01 sequence band of the CO_2 laser frequencies in MHz [2].

J	P branch			R branch		
	00^01 ref. line	Observed IF = $\nu_s - \nu_r$	Calculated 00^02 freq.	00^01 ref. line	Observed IF = $\nu_s - \nu_r$	Calculated 00^02 freq.
11	P14	+ 6579.4	28471254.4	R8	– 10288.3	29000850.8
13	P16	+ 8120.9	28420711.3	R10	– 11687.3	29042389.9
15	P18	+ 9675.3	28369449.5	R10	+ 29128.7	29083200.0
17	P20	+ 11245.3	28317468.1	R12	– 14452.9	29123278.8
19	P20	– 41464.7	28264766.1	R14	+ 24887.9	29162623.6
21	P22	– 40600.8	28211342.4	R16	+ 22775.9	29201231.7
23	P24	– 39728.6	28157195.3	R18	+ 20667.8	29239100.2

band laser is equipped with an internal CO_2 hot cell to suppress the regular band lines. The reference laser operates on regular band lines. The internal fluorescence CO_2 cell is placed in the reference laser cavity, to distinguish the sequence band lines from regular ones (the sequence lines are not absorbed in the CO_2 cell and do not show fluorescence). The reference and the sequence laser beams are focused onto a tungsten-nickel diode. The different frequencies can be directly measured with a spectrum analyser. When the difference frequencies are above 3 GHz, they can be additionally mixed with microwave frequencies of the klystron (8290, 10000 or 12005 MHz or one of their harmonics up to the fifth). The frequencies thus converted down (below 3 GHz) are phase-locked to a 5 MHz signal from ^{133}Cs standard. The frequencies are measured by comparison with the known marker frequency on the spectrum analyser. In Table 2 some chosen sequence frequencies are shown [2]. The observed intermediate frequencies between sequence ν_3 and regular ν_r frequencies of *P* and *R* branches are the base to calculate the absolute frequencies of the sequence 00^02 lines.

4.3. Simple heterodyne analysis of the laser emission line spectral contents

Spectral contents of the laser output beam can be easily observed using an additional single-mode laser as a reference source. Heterodyning both laser beams on the photo -detector we can observe beat frequencies at the scope, when both lasers operate at

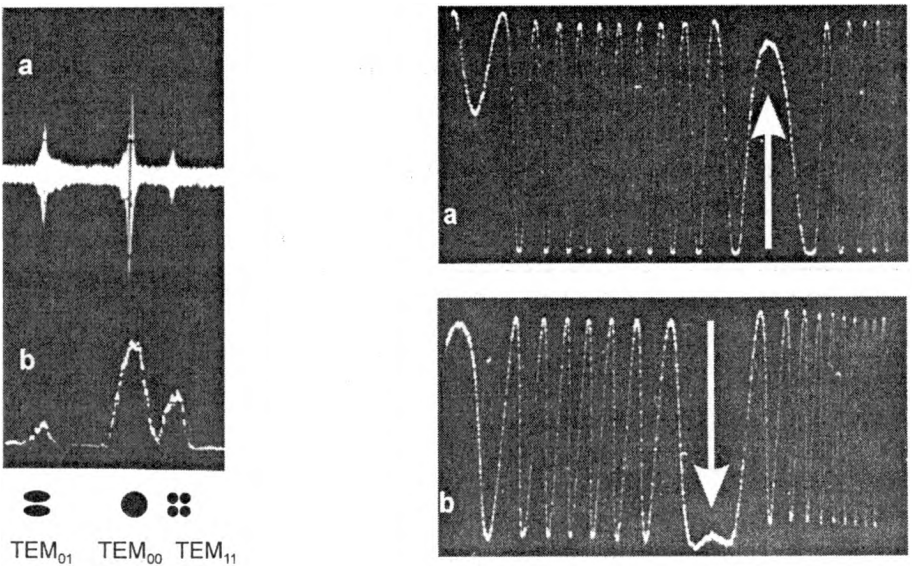

Fig. 6. Beat frequency signal obtained by heterodyning the single-mode CO_2 laser (**a**) and three-mode CO_2 laser [34] (**b**). Three modes are detected as a beat signal (**a**) and classical perturbations in the shape of the gain curve (**b**).

Fig. 7. Zooms of the beat frequency signals of two CO_2 lasers(**a**, **b**). Arrows indicate two moments when frequencies of both lasers "meet" together [35].

almost the same frequency (it means, when the beat frequency does not exceed the frequency range of both the scope and the detector). An example is given in Fig. 6. One of the lasers was a single-mode one and it was used as a reference source. The second laser has operated (as it seen in the figure) in three modes: TEM_{00}, TEM_{01} and TEM_{02} (Fig. 6**b**). Both CO_2 lasers have operated on the same P20 line selected with a diffraction grating. The beat frequencies registered in Fig. 6**a** have been obtained by tuning the laser using the piezoelectric transducer. Each time one of the modes of the laser was close enough to the frequency of the source laser, the beat frequency signal was observed.

It can be interesting to see a zoom of the beat frequency signal. When both lasers operate at the same frequency, then no beats are expected. We can see such a zoom in Fig. 7**a**, **b** [35]. When the frequency of the tuned laser becomes equal to the frequency of the source laser, the zero beat signal is observed (see arrows in the figures).

4.4. Heterodyne analysis of the laser radiation in pulse regime

The method will be demonstrated here using a RF excited slab-waveguide CO_2 laser. Output pulses from RF excited lasers are relatively long compared to TEA lasers, where input energy is collected in capacitors and suddenly dissipated into an active laser mixture. The pulse regime of the RF excited lasers should rather be called a periodical -pulse operation. This is because of the specific excitation of the lasers. The input RF switching pulse from the power oscillator releases the output pulse of the radiation,

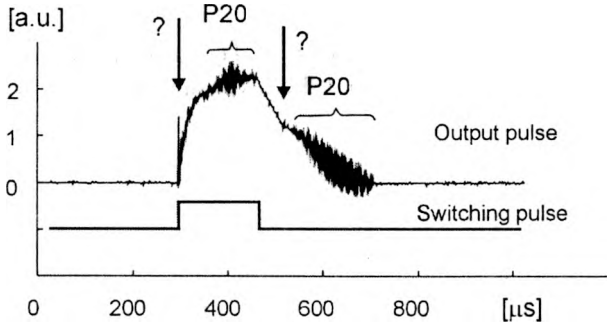

Fig. 8. Output laser pulse from the slab-waveguide CO_2 laser in pulse regime. Laser jumps from one emission line to another during the pulse duration [36].

where only first, short part (called a gain switching) is sharp and relatively high in comparison with the further part of the developed pulse shape. Figure 8 shows a typical output pulse of the radiation from the slab-waveguide laser [36]. As it is seen, the switching gain pulse is generated as the first one, and in the next step the laser operates in steady state conditions. In the meantime, it jumps from line to line. The picture was obtained using the heterodyne method. The shape of the output pulse is disturbed with the beat signal obtained by heterodyning of the investigated slab-waveguide laser with a cw single-mode CO_2 laser. The signal appears two times during the pulse evolution.

It means that the laser pulse has started from one, unknown line (indicated in Fig. 8 as "?"), and next it has jumped onto P20 line. When the switching pulse has been switched off, the laser in natural way "returned" to the same, P20 line. The heterodyning method gives a very clear picture of the phenomenon under investigation.

Heterodyne analysis is quick enough to investigate even short laser pulses. It is easy to show that output pulses of TEA CO_2 lasers are generated on one, chosen emission line [37].

4.5. Homodyne analysis of the laser emission line spectral contents

The homodyne method does not require any additional single-mode laser. The intermode beats of the chosen laser can be easily investigated with the method. For instance, observed in Fig. 6 three modes beat together and give as a result the beat frequencies on the photodetector. Using a spectrum analyser one should observe three peaks responsible for the difference frequencies: $\nu_{TEM_{01}} - \nu_{TEM_{00}}$, $\nu_{TEM_{02}} - \nu_{TEM_{00}}$, $\nu_{TEM_{01}} - \nu_{TEM_{02}}$, on the analyser screen. The example of the homodyne detection of the RF excited waveguide CO_2 laser is shown in Fig. 9. Seven beat frequencies have been observed as a result of the analysis: 4, 18, 60, 64, 78 and 82 MHz. A simple analysis of the results brings about the solution of the "puzzle". The frequencies of high order modes in waveguide laser cavity can be expressed by the simplified formula

$$\nu_{j,mn} \approx \frac{jc}{2L} + \frac{c\lambda}{32}\left(\frac{m^2}{a^2} + \frac{n^2}{b^2}\right) \tag{5}$$

where: j – number of the longitudinal mode, m, n – range of the EH_{mn} mode, a, b, L – dimensions of the laser waveguide, c, λ – light speed and the laser line wavelength, respectively.

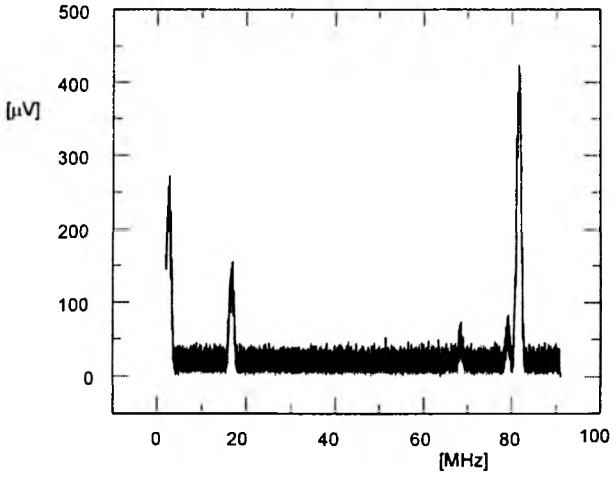

Fig. 9. Inter-mode beat frequencies ("hooting" modes) of a RF excited waveguide CO_2 laser (60 MHz beat is not visible in the figure) – see the explanation in the main text [38].

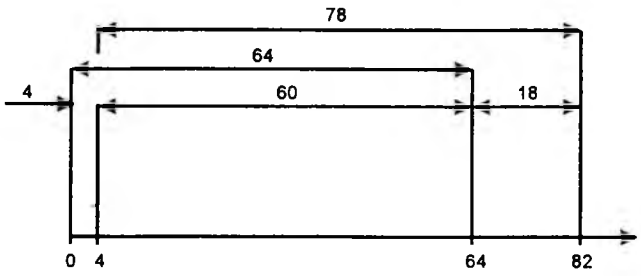

Fig. 10. Explanation of Fig. 9. Possible beat frequencies between four laser modes (in MHz).

The above-mentioned combination of the beat frequencies can fulfil four modes: $\nu + 0, + 4, + 64$ and $+ 82$ MHz, where ν – some frequency around the central frequency of the CO_2 emission line emitted by the laser (see the explanation in Fig. 10). The intermode beats, observed as a spectrum in Fig. 9, are the result of beatings between so-called "hooting" modes that are parasitic and difficult to avoid in waveguide lasers [3]. The phenomenon observed is caused by non uniformity of waveguide side-walls (see values a and b in expression (5)). It has been pointed out that beats caused by "hooting" modes usually do not exceed 100 MHz [3], [38].

5. Signatures

The longitudinal resonance frequencies of the laser resonator are separated by the so-called free spectral range (FSR)

$$\Delta\nu_{FSR} = \frac{c}{2l} \tag{6}$$

where c – speed of light.

For example, for the resonator $l = 1$ m long the distance $\Delta\nu$ between two adjacent longitudinal modes is equal to 150 MHz. For all types of CO_2 lasers which operate at higher pressures than 1 Tr, the gain line is homogeneously broadened. It means that whatever the length of the resonator and gain line width, such a laser always operates in longitudinal mode. However, the laser can operate simultaneously in more than one transverse mode if only it has spatial conditions to form higher-order transverse modes. One basic longitudinal mode fully saturates the homogeneously broadened line in its modal volume and it does not give any chance to excite any other longitudinal modes. Transverse modes use different unsaturated modal space and if they have space, they can oscillate inside the laser resonator, simultaneously with other different transverse modes. Higher order transverse modes can be suppressed by putting a diaphragm inside the resonator. In that way, one basic longitudinal mode is selected, and the laser operates as a single mode and single frequency laser. However, when the resonator is tuned along its FSR, the laser resonances overlap different CO_2 vibrational-rotational emission lines. As a result, the laser line jumping occurs during the process of tuning.

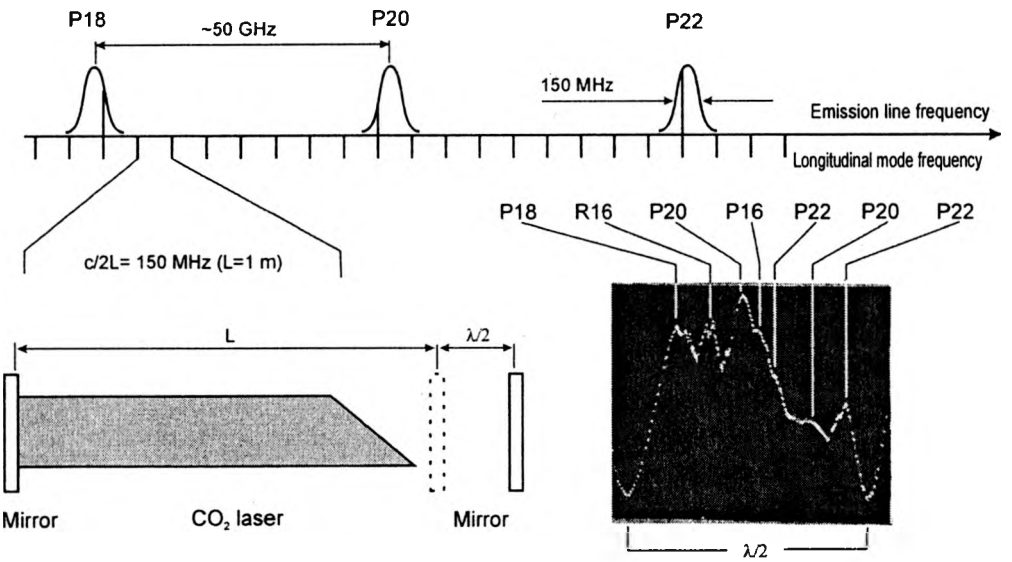

Fig. 11. Explanation of signature forming: top – distribution of laser emission lines and longitudinal modes; left – the scheme of the laser equipped with a resonator of length L with possibilities to tuning of $\lambda/2$; right – the signatures of the CO_2 laser [35].

The phenomenon is called a signature of the laser. So, the signature depends on the length and structure of the resonator, and type of the CO_2 laser. That is a very specific phenomenon for the CO_2 lasers.

Figure 11 shows a signature of the cw CO_2 laser obtained by tuning the resonator of one-half wavelength. A few laser emission lines are responsible for the maximum of the signatures. They seem to appear unpredictable. Actually they appear according to some rules depending on the length of the laser resonator [39], [40]. It is possible to obtain simultaneous oscillation of the cw CO_2 laser on a few rotational lines – so-called "multi-colour" operation for some geometrical conditions with careful tuning control and mode selection [41]. Simultaneous multi-colour operation is also possible in pulsed regime of the TEA CO_2 lasers [42].

5.1. Well-ordered laser signature (WOLS effect)

Usually emission lines in the signature do not follow the natural order of the CO_2 molecule emission spectrum. However, in some cases, especially in lasers equipped with unstable resonators, emission lines appear in the signature exactly in the natural order of CO_2 emission spectrum. It is so-called WOLS effect (well-ordered laser signature) [43]. Figure 12 illustrates this case for the slab-waveguide RF excited CO_2 laser equipped with an unstable positive branch resonator in open structure, that is, without sidewalls. The open structure is an important element of the laser system here, otherwise higher order modes can be excited, and as a consequence the laser signature becomes very complicated and unpredictable. As can be seen from the figure, even

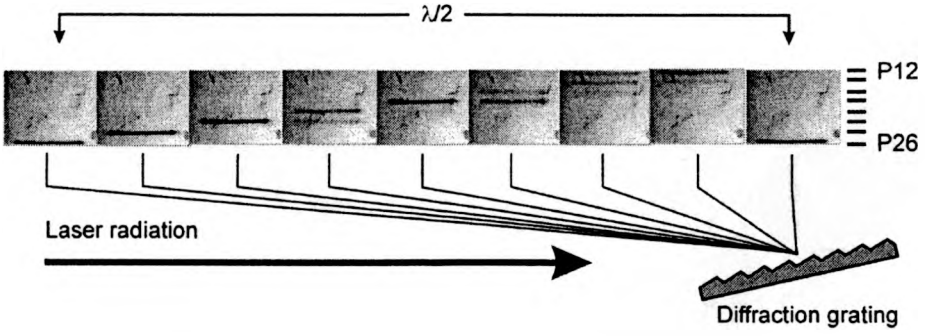

Fig. 12. Well-Ordered Laser Signature (WOLS) of the slab-waveguide CO_2 laser [43]. The picture registered on the UV screen. Spectral analysis is performed using a diffraction grating as a analyser. The laser exhibits the well-ordered signature containing 8 emission lines from P12 to P26 lines of the 10.4 μm band. The length of the resonator L is approx. 402.6 mm.

eight emission lines from the P branch can be observed line by line according to the natural order of the CO_2 emission spectrum. This phenomenon is easily observable in CO_2 lasers with unstable resonators due to a low Q-factor of the resonant cavity.

5.2. Diffractive scanning mechanism for a laser marker

One of the technological applications of CO_2 lasers is marking. Usually, the output laser beam is controlled using a system of movable mirrors to obtain a required sign on a target. In that way it is possible to draw any figures and signs with a continuous line. Another solution is a dot marker, where required shapes are formed by a series of dots. A good solution is choosing the multiwaveguide CO_2 laser, where each output

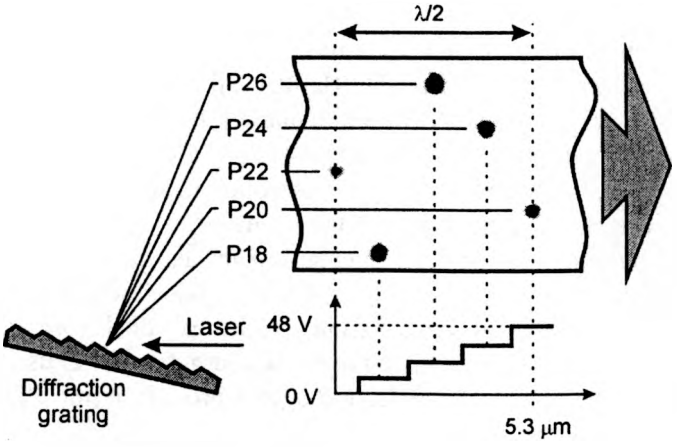

Fig. 13. Spectral analysis of the CO_2 laser radiation with a diffraction grating. (A single RF excited waveguide CO_2 laser with dimensions of 2.5×2.5×400 mm^3 was used). Levels of the voltage on the PZT are indicated [45]. The laser exhibits the quasi-chaotic signature of P18, P20, P22, P24 and P26 emission lines of the 10.4 μm band.

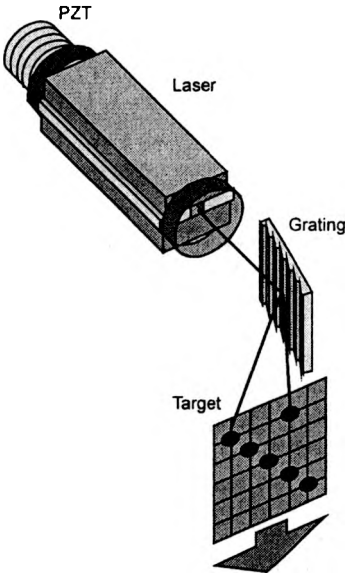

Fig. 14. Idea of the laser diffraction marker. A piezoceramic transducer (PZT) and a diffraction grating are executive elements of the marker. A target is movable in one direction. (The main shutter is not indicated in the picture) [4].

beam is chopped and a target periodically moved [44]. But there exists another solution. When the beam from the single-tube or single-waveguide laser is deflected on the diffraction grating and then directed to the movable target, series of specifically distributed spots can be observed as well. Figure 13 shows the result of such a spectral analysis [45]. The signature of the laser is represented by a series of dots distributed in a quasi-chaotic way. It is very well known that the signature of the CO_2 laser is stable and repeatable with each half-wavelength for the given length of the optical resonator. The signature can be very easily predicted [39], [40].This representation of the signature can be the basis for designing a dot diffraction marker. Figure 14 presents the idea of the dot type marker based on spectral properties of the CO_2 laser radiation [4]. Positions of the marked points on the target can be controlled using appropriate voltage on the piezoceramic transducer, as is shown in the figure.

The diffraction marker does not use movable elements such as galvanometer mirrors or sophisticated systems of shutters, in comparison to classical solutions of the laser markers presented above. As usual, the efficiency and speed of the present method of marking depend on both the output laser power and target material used. Another parameter influencing the speed of the technological process is the PZT inertia.

Application of the slab waveguide laser (in unstable configuration) to dot markers can be of much use. The laser exhibits much higher level of the output power and the WOLS effect (see the last subsection). In this way, the controlling of the output beam can be very clear.

5.3. Multi-waveguide laser

One-dimensional or two-dimensional CO_2 laser arrays are a very efficient source of the laser radiation. Two-dimensional arrays exceed 1 kW output level [46]. Additionally, using some reformatting beam techniques, they can give an output beam with quite a high quality (low M^2 parameter) [5], [47]. Figure 15 shows the result of spectral analysis of the one-dimensional eight-waveguide RF excited CO_2 laser. It has been checked that each channel of the laser operates independently [48]. Figure 15**a** shows a very rare case where all channels work simultaneously on P20 emission line (a very difficult case to control). Another example can be seen in Fig. 15**b**, where the

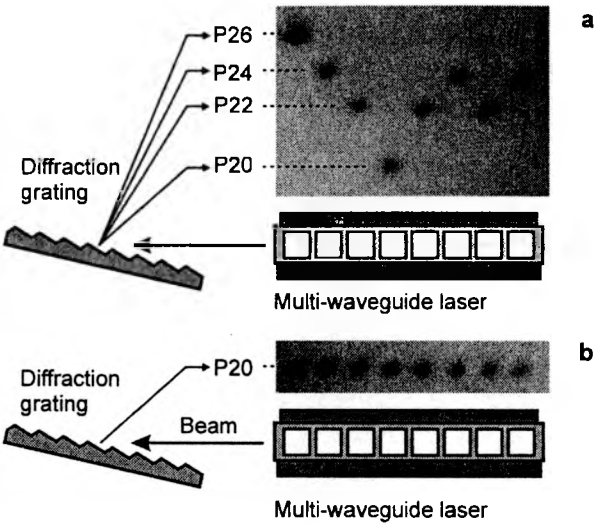

Fig. 15. Spectral analysis of an eight-waveguide RF excited CO_2 laser. **a** – all channels operate on the same P20 emission line (very rare case), **b** – output radiation dissipated chaotically into a few emission lines from P20 to P26 (common case).

sign of the shape of "Cassiopeia" was obtained accidentally and it was not repeatable. The reason for observed "dissipation" of the laser beams into different emission lines is a very low phase coupling between separate channels. For a typical multi-waveguide array with dimensions of $2\times2\times400$ mm^3 the coupling does not exceed the value of 0.6 MHz [48]. Thus, reconfiguration of the dot marker based on a multi-waveguide laser into a diffraction marker can be difficult.

5.4. Pulse operation

The line jumping is particularly difficult to control for pulse laser operation cases. The injection of pulse power into the gas discharge implies strong plasma heating, consequently changing the refractive index, which, as a result, causes dynamic detuning of the laser spectrum throughout the pulse duration [49]–[51]. It has already been mentioned that the jumps are easy to monitor using the heterodyning method.

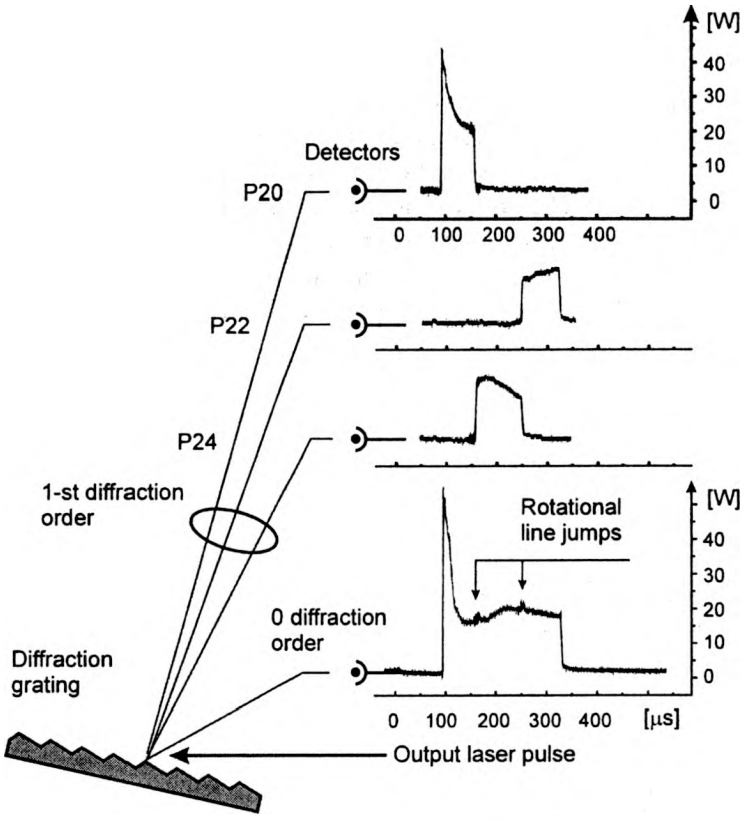

Fig. 16. Spectral analysis of the CO_2 laser pulse. The single-waveguide RF excited CO_2 laser was used in the experiment [51].

Another way is to use the experimental setup with a diffraction grating, like that presented in Fig. 16. It consists of an external diffraction grating, fast HgCdTe photodetectors and a digital scope. The diffraction grating deflects the spectral lines. One photodetector registers the total shape of the output pulse (zero diffraction order) and the other one (first diffraction order), settled behind the grating in the reimage plane, detects the pulse shape of the selected line. This system was allowed to register the pulse evolution of all oscillating spectral transitions contributing to the total shape of the output pulse. The results are shown in Fig. 16. The phenomenon was examined on an RF excited CO_2 single waveguide laser [51]. The laser of a $2\times2.5\times380$ mm^3 waveguide channel was driven with the RF 125 MHz frequency. A typical profile of the output laser pulse is shown in Fig. 17. It consists of the high and narrow peak (gain switching) and next the flat region responsible for the cw operation. The output pulse starts after some delay time $\Delta\tau$ (in relation to the beginning of the switching input pulse), necessary for pumping the laser medium and developing the plasma in the laser

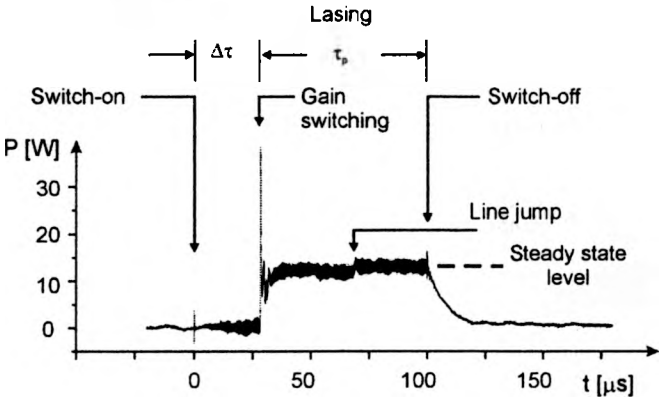

Fig. 17. Laser output pulse structure formed when the input power is switched on and off. The result obtained for a RF excited single-waveguide CO_2 laser [7], [51].

channel. The perturbations shown on the flat part of the pulse are caused by rotational line jumping due to the plasma heating effect. The sequence of jumping lines can be used for estimation of changes of the mean temperature and pressure of the laser plasma throughout the pulse.

In Figure 18, one can see rough estimations of changes of the plasma temperature and pressure with the evolution of the pulse. The laser medium was pumped with the input power of 750 W at a pressure of 80 Tr. If the temperature is too high, *i.e.*, when plasma is overheated, the laser output pulse is shortened, as shown in Fig. 18, and the temperature bulge is observed [7]. Depending on conditions (mainly the level of the RF input power) the line hoppings from 1 to 5 lines throughout the pulse duration are observed.

The present method is useful for diagnostics of the laser plasma in dynamic conditions. Several assumptions were made when constructing the characteristics in Fig. 18. First, it was assumed that both temperature T and pressure p of the laser medium grow simultaneously (up to 650 K and 180 Tr, respectively) fulfilling an isochoric process. The strong compression in the laser channel occurs but a refractive index n of the medium does not change: the laser operates in the meantime on one chosen emission line (the first spike called gain switching). In the next part of the pulse, the temperature T can still rise or drop depending on the supplying conditions. In the meantime, decompression process occurs, density N of the laser gas decreases, and the refractive index drops according to the equation of state of an ideal gas

$$N = \frac{p}{kT}. \tag{7}$$

The laser detunes, and as a consequence the line hoppings are observed. Detailed explanation is provided in the caption to Fig. 18.

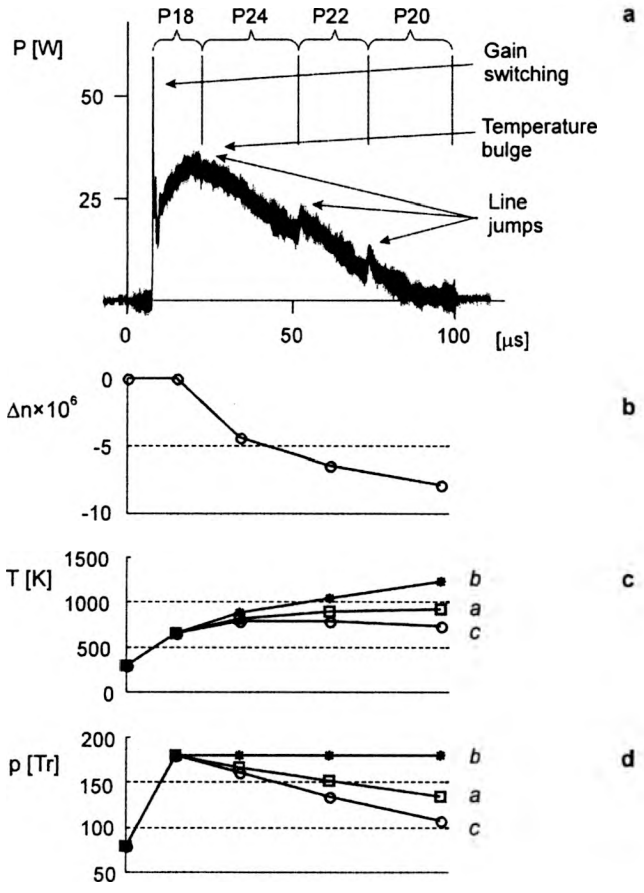

Fig. 18. Explanation of the line jumping phenomenon in the CO_2 laser in pulse regime. **a** – output laser pulse at the input power of 750 W. The sequence of P18, P24, P22 and P20 lines is visible. The laser mixture is overheated, and the temperature bulge occurs on the shape of the pulse; **b** – relative changes of the refractive index Δn vs time. The index does not change during the first part of the pulse (gain switching) – then isochoric process occurs; **c** – temperature changes T vs time. The temperature at the beginning was established as 288 K. Next point (gain switching) was assumed as 700 K; **d** – pressure changes p vs time. The pressure at the beginning was established as 80 Tr. Next point (gain switching) was assumed as 180 Tr. The characteristics T (time) and Δn (time) are the consequence of the assumed data points. Three sets of assumptions were taken into account: a – the temperature remains constant, b – rises, and c – drops.

It is easy to notice that the number of the line hoppings in single-channel laser is higher than in the case of the slab-waveguide (*cf.* Figs. 8 and 18). In the slab conditions, the compression of the gas mixture at the beginning of the pumping pulse is much lower than that in a single-channel waveguide laser with sidewalls. On the other hand, the decompression is higher due to the free space in the slab-waveguide (lack of sidewalls). As a consequence, changes of the refractive index are smaller. Thus, only two emission lines are generated over the pulse duration in typical ($2\times40\times400$ mm^3) open structures of the slab-waveguide lasers [36].

6. Optical pumping-lasers operating in submillimeter region (FIR lasers)

Operation of the far infrared (FIR) laser is based on the coincidence absorption lines of the FIR laser medium with source laser lines. The CO_2 laser is particularly suitable for optical pumping of the FIR laser media. Many heavy molecules like methyl fluoride (CH_3F), or ethanol (C_2H_5OH), or methanol (CH_3OH), and many other molecules have absorption spectrum close to the 10.6 μm or 9.6 μm bands of the CO_2 laser [52]. In the first reported paper about the optically pumped submillimeter laser, methyl fluoride gas was used as an active FIR laser medium [53]. The 9.55 μm wavelength of a P20 emission line of a 9.4 μm CO_2 laser band just suits the resonance absorption $\nu_0 \rightarrow \nu_1$ modes of the CH_3F molecule. Six rotational transitions around 452, 496 and 451 μm were observed. The Q-switched CO_2 laser was used as pumping source. Figure 19 illustrates schematically the idea of the laser optical pumping and the FIR laser action.

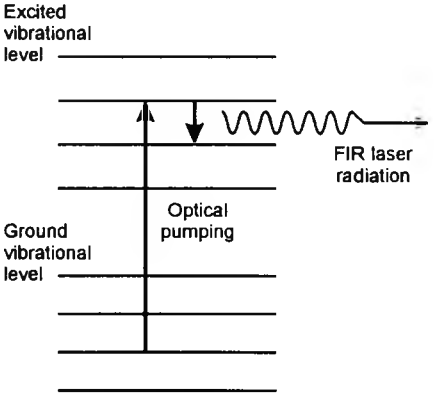

Fig. 19. Scheme of the optical pumping in submillimeter lasers. Pumping energy is much higher (short wavelength), output radiation is emitted as a long wave.

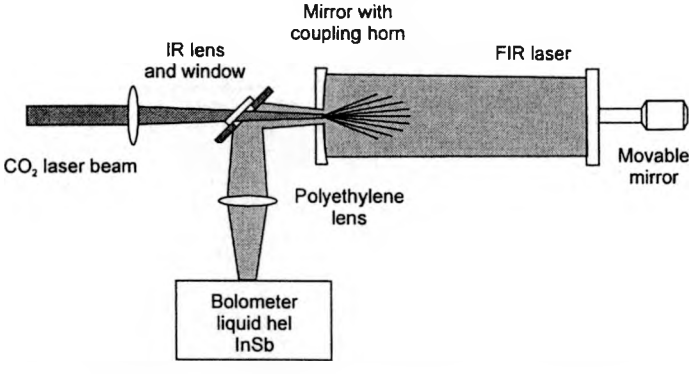

Fig. 20. Scheme of the first, Chang–Bridges construction of the optically pumped CH_3F submillimeter laser [53].

Figure 20 shows schematically the first, Chang–Bridges construction of the optically pumped CH_3F submillimeter laser [53]. The CO_2 laser radiation is delivered to the FIR chamber through the infrared window (transmitting for a CO_2 laser beam), and it is dissipated into the methyl fluoride. The coupling horn is used for better dissipation of the beam. The submillimeter radiation leaves the FIR chamber, and it is directed through the polyethylene lens (transmitting for a FIR laser beam) to the detector.

6.1. Double optical pumping

One of the more interesting methods of the optical pumping of the FIR laser medium is a double pumping. Figure 21 illustrates schematically the idea. The NH_3 FIR laser medium is pumped simultaneously with two CO_2 lasers [54]. One of the lasers is tuned to the transition $(0^-, 5, 3) \rightarrow (1^+, 5, 3)$ of the NH_3 level of the ν_2 mode, and the second one to the transition $(1^+, 4, 3) \rightarrow (2^-, 5, 3)$ of the same NH_3 mode. The first

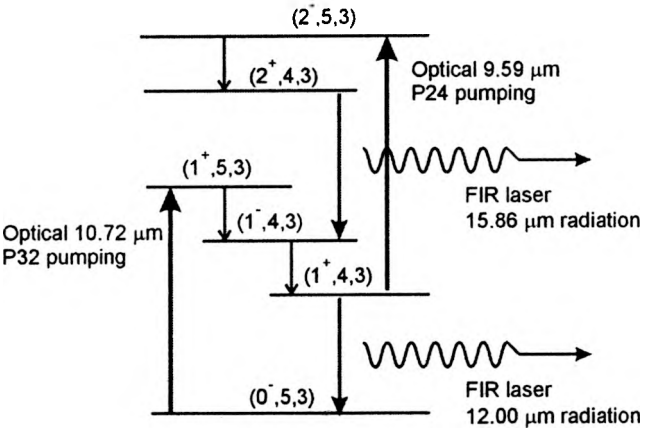

Fig. 21. Simplified diagram of the NH_3 FIR laser transitions of the n_2 mode pumped with two CO_2 laser wavelengths of P32 (10.4 μm band) and P21 (9.4 μm band) [54].

T a b l e 3. Transitions of the duble pumped NH_3 FIR laser [54].

Wavelength [mm]	Transition
12.00	$(1^+, 4, 3) \rightarrow (0^-, 5, 3)$
13.23	$(2^+, 6, 3) \rightarrow (1^-, 5, 3)$
13.66	$(2^+, 5, 3) \rightarrow (1^-, 4, 3)$
15.78	$(2^+, 5, 3) \rightarrow (1^-, 5, 3)$
15.86	$(2^+, 4, 3) \rightarrow (1^-, 4, 3)$

laser operates on a P32 emission line of the 10.6 μm branch, the second one operates on a P24 emission line of the 9.4 μm branch. As a result, the FIR radiation on the 15.86 μm wavelength is emitted (transition $(2^+, 4, 3) \rightarrow (1^-, 4, 3)$). Also other transitions are possible, as collected in Tab. 3, and not indicated in Fig. 21 [54].

6.2. Off-resonance pumping

The most effective optical pumping occurs upon the strict coincidence of both absorption (FIR) and emission (pumping source) line centres. Usually, the CO_2 emission is not resonant with the vibrational absorption, although some inversion of the FIR medium occurs. It was observed that an off-resonance pumping in ammonia molecule shows even a several gigahertz mismatch between the centres of the absorption peak and laser pumping line [55]. The off-resonance pumping increases the number of useful submillimeter lines. But for the efficient pumping, some techniques of the mismatch reduction between pumping and absorption lines are necessary [56].

6.3. Frequency displacement techniques of pumping

One of the active frequency displacement techniques is application of the Stark effect in the FIR medium. It that way, instead of the pump frequency displacement, a displacement of the absorption line is obtained. The technique used for ammonia medium (NH_3) gave the displacement of the absorption line of 10–100 MHz for Stark fields of a few kV/cm [57].

Other displacement techniques are based on the proper translation of the centre of the CO_2 pumping lines in relation to the centres of the absorption FIR lines. In practice, acousto-optic or electro-optic modulation techniques are applied [58],[59].

In some cases, a suitable displacement of the CO_2 laser frequency can be easily obtained tuning the laser resonator [60]. A high tunability of the laser can be achieved increasing the pressure of the CO_2 medium. The bandwith of the CO_2 laser can exceed the value of 1 GHz in waveguide conditions (with relatively high pressure up to 200 Tr), which involves the tunability of more than 2 GHz using a CdTe etalon [61], [62].

The main advantage of the FIR laser is the emitted wavelength, thus applications to spectroscopy [63]. A long wave is easily deflected, thus very useful for plasma investigation [64]. So far wavelengths are emitted from the FIR lasers because of the short energy distance between lasing levels in heavy molecules. The property of long wavelength operation is common for most of the FIR lasers. There have been observed the wavelengths from 0.04 to 2 mm [52]. The CO_2 laser with its spectral properties is an important element of the FIR laser systems.

7. Methods of CO_2 laser spectrum spreading

The spectrum of the CO_2 molecule enables operation of the laser on many emission lines at strict frequencies. There are a few methods for spreading available spectrum of the CO_2 laser:

– forcing the laser to operate on sequence bands using a hot absorber,

– by optical pumping sequence levels, by selective electronic-to-vibrational energy transfer,

– using isotopes C^{12} or O^{16} (or both).

These methods allow the laser spectrum to be spread from 9 to 16 micrometers.

7.1. CO_2 laser operation in the 9–11 μm region. Sequence bands

The common 10.4 μm or 9.4 μm bands of the CO_2 laser emission spectrum are the consequence of the so-called "regular" transitions between either 00^01 and 10^00 or 00^01 and 02^00 levels (see Fig. 22). The regular bands consist of *P* and *R* branches with alternate *J* values missing. However, a rich scheme of the energy levels of CO_2 molecules gives other possible transitions from higher levels, such as 00^02 or 00^03. The rotation-vibration transitions $00^02 - (10^01, 02^01)_I$ and $00^02 - (10^01, 02^01)_{II}$ give the so-called "sequence" bands. They are very similar in their structure to regular bands but, in contrast, they contain only odd *J* values in the lower level. The frequencies of the transitions are translated slightly in relation to the regular bands because of the small anharmonicity of the CO_2 molecule. The sequence transitions can be observed in a conventional low pressure CO_2 laser, but to separate them from the much stronger regular transitions, it is necessary to place an etalon in the laser cavity [61]. Another,

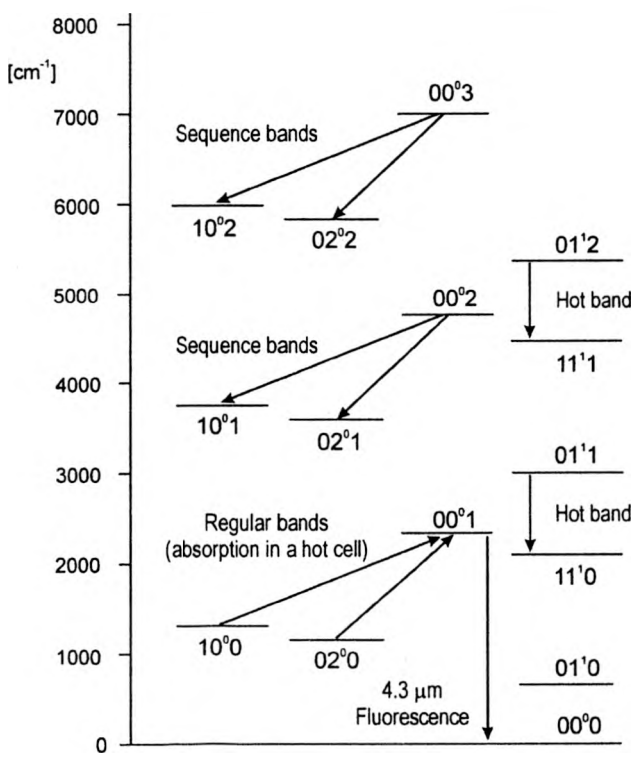

Fig. 22. Vibrational energy level diagram of CO_2 with regular, hot and sequence bands [8], [9].

most efficient, method is to put an internal absorption cell in the laser resonator filled with hot carbon dioxide gas. Such a laser operates only on the sequence lines [10], [11]. The method is simple. The lower levels of the regular bands lie relatively close to the ground state and they have an appreciable thermal population, particularly when the CO_2 is heated. As a consequence, all the regular laser lines show absorption in hot CO_2. In that way, sufficient loss is introduced into the mechanism of lasing which causes suppression of the regular laser oscillations. Thus, the laser operation can only take place on the sequence bands. The lower level in the sequence transitions lies far above the ground state and therefore they give no fluorescence signal in the CO_2 absorption cell. It is a very simple method of distinguishing between regular and sequence bands.

Recently, the other hot band lines have been found in a classical cw CO_2 laser without any additional arrangements, such as CO_2 absorption cells. There have been observed lines from the region of 9 μm, very interesting for optical pumping of methanol and difluoromethane FIR lasers [12].

7.2. Electronic-to-vibrational energy transfer as a pumping mechanism. The 14.1 μm Br^*-CO_2 laser operation

Electronic-to-vibrational energy transfer (E-V) from an excited Br_2 molecule to a CO_2 molecule as a pumping mechanism is one of the sophisticated methods of excitations of upper CO_2 laser levels [13]. Direct transfer from the excited Br^* level to the 10^01

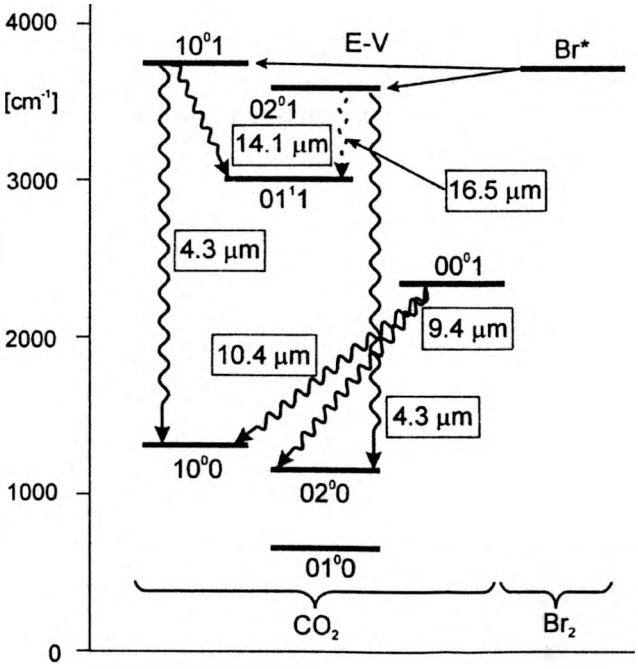

Fig. 23. Energy-level diagram of the Br^*-CO_2 system [13].

level of the CO_2 causes stimulated emission either from 10^01 to 10^00 or from 02^01 to 02^00 CO_2 levels known as laser outputs at 4.3 μm. Apart from that, stimulated emission from 10^01 to 00^11 levels at 14.1 μm can be observed. Regular transitions either from 00^01 to 10^00 or from 00^01 to 02^00 at 10.4 μm and 9.4 μm are also observed. Figure 23 illustrates the energy transfer mechanism and possible stimulated transitions.

7.3. Isotope shift

The spectrum of a molecule depends on its structure and mass of all its atoms. The mass of a molecule can be changed by replacing atoms with their isotopes, without changing the structure of the molecule. In the case of the CO_2 molecule, carbon and oxygen atoms can be changed into their isotopes. Instead of basic ^{12}C and ^{16}O atoms, their isotopes ^{13}C or ^{14}C and (or) oxygen isotopes like ^{17}O and ^{18}O can be used. Mode frequencies ω_1 – symmetric, ω_2 – bending and ω_3 – asymmetric after isotopic substitution are modified according to the formula [17]

$$\frac{\omega_1^i}{\omega_1} = \sqrt{\frac{m_O}{m_{O^i}}}, \qquad \frac{\omega_2^i}{\omega_2} = \frac{\omega_3^i}{\omega_3} = \sqrt{\frac{m_O\left(1+\dfrac{2m_{O^i}}{m_{C^i}}\right)}{m_O\omega\left(1+\dfrac{2m_O}{m_C}\right)}} \tag{8}$$

where: m_O and m_C – the masses of the oxygen and carbon atoms, i refers to the isotopic species.

Eight combinations of the CO_2 molecule were investigated as a component of the CO_2 laser mixture: $^{12}C^{16}O$ (basic), $^{13}C^{16}O$, $^{14}C^{16}O$, $^{12}C^{16}O^{18}O$, $^{13}C\,^{16}O^{18}O$, $^{12}C^{17}O$, $^{13}C^{18}O$ and $^{14}C^{18}O$. The CO_2 laser basic and isotopic transitions give the spectrum from 9 μm to 12 μm [14]–[17]. It is easy to notice that a carbon isotope has the strongest

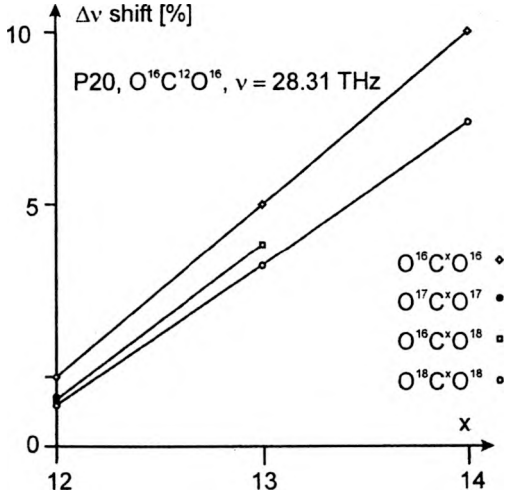

Fig. 24. CO_2 isotope shifts for the P20 line of the CO_2 laser regular band.

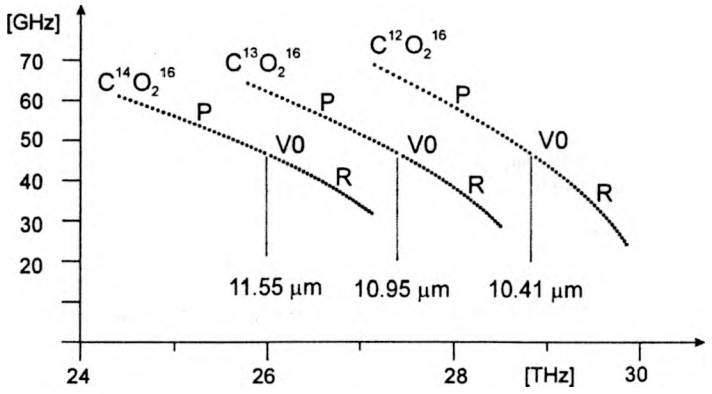

Fig. 25. CO_2 isotope shifts of the CO_2 laser 10.4 μm regular band for three isotopes ^{13}C (centre) and ^{14}C (left). Basic band is indicated for ^{12}C (right).

influence on the spectrum. Figure 24 shows that carbon isotopes can translate the centre of a P20 CO_2 line even by 10%. Figure 25 shows how a 10.41 μm basic spectrum of the carbon dioxide laser can be translated to 10.95 μm and 11.55 μm for additions of ^{13}C and ^{14}C isotopes, respectively.

8. Frequency fluctuations of the CO_2 laser radiation

The spectral intrinsic width $\Delta\nu_i$ of the output laser radiation is very narrow and can be expressed by a Schawlow–Townes formula [65]

$$\Delta\nu_i = \frac{2\pi(\Delta\nu_c)^2 h\nu_0}{P_{\text{out}}} \tag{9}$$

where: Δn_c – spectral width of the passive resonator, ν_0 – frequency of the line centre, P_{out} – output power.

Putting typical data into the Schawlow–Townes formula, $\Delta\nu_c$ = 5 MHz, P_{out} = 10 W, ν_0 = 28 THz, the intrinsic width of CO_2 laser radiation is in the range $\Delta\nu_i \approx 10^{-6}$ Hz. It is a very narrow line, and its relative instability $\Delta\nu_i/\nu_0$ is very low, on the level of 10^{-18}, which makes such a laser a potential standard of frequency. Figure 26 illustrates relations between widths of the laser spectral line, the passive resonator line and the intrinsic width of the output laser line. However, one has to remember that there is a strong fluctuation process in the laser resonator caused by environmental fluctuations and the real width of the laser radiation is by a few orders higher. There are two main sources of laser frequency fluctuations described by the formula

$$\nu_0 = q\frac{c}{2n_0 l_0} \tag{10}$$

where: n_0 – refractive index of the laser medium, l_0 – length of the laser resonator.

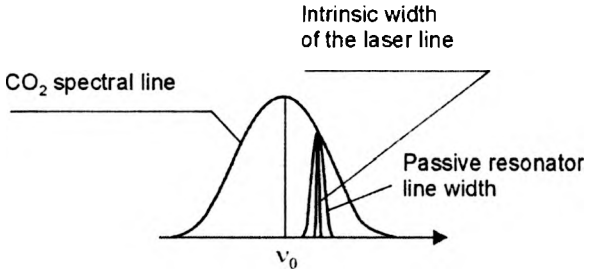

Fig. 26. Comparison of the spectral width of the laser output radiation, passive resonator line and spectral line.

The refractive index $\Delta n(t)$ changes, and the length of the resonator $\Delta l(t)$ changes result in frequency fluctuations of the laser according to the transformed formula from (10)

$$\Delta\nu(t) = -\frac{\nu_0}{n_0 l_0}[n_0 \Delta l(t) + \Delta n(t) l_0]. \tag{11}$$

8.1. "Blue" and "red shift"

Changes of the refractive index $\Delta n(t)$ are caused by such phenomena as changes of pressure, temperature, chemistry of the plasma, pulling frequency effects. For example, the dc excited CO_2 laser shows 0.5–1 MHz/mA of "blue shift" of the oscillating frequency due to change of the discharge current I [18]. Also "red shift" of the central frequency is possible due to changes of pressure p, see Fig. 27. For RF

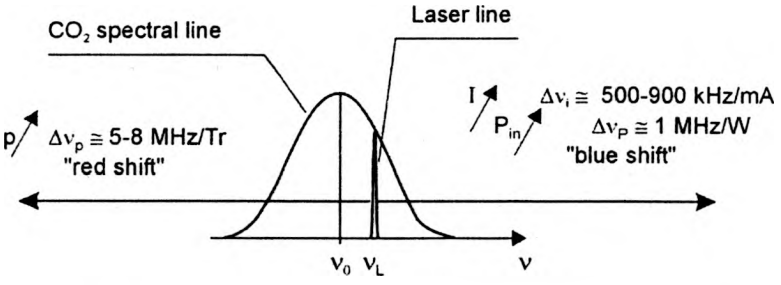

Fig. 27. Effects of "blue" and "red shift" of the CO_2 laser line ν_L, in the range of the gain curve width ν_0, due to pressure p ("red shift"), dc current I ("blue shift") and RF input power P_{in} ("blue shift").

excited CO_2 lasers an increase of the input RF power causes "blue shift" of frequency operation with sensitivity 1 MHz/1 W [19]. Changes of the laser resonator length $\Delta l(t)$ are caused by temperature drifts, mechanical and acoustic vibrations, and they can be compared with FSR (free spectral range).

8.2. Pulling effect

The influence of the gain line shape on the laser frequency is called the pulling effect. It manifests itself in that the shape of refractive index around the spectral line changes and the shape follows the first derivative of the spectrum line, and its value depends on the gain (see additional explanation in Fig. 28). In that way, the frequency of the passive resonator differs from the laser frequency: the frequency of the laser is "pulled" to the centre frequency of the emission line. That frequency pulling shift $\Delta\nu_p$ can be expressed by simplified formula [65] valid around the central line

$$\Delta\nu_p = (\nu_0 - \nu_L)\frac{\Delta\nu_c}{\Delta\nu_h} \tag{12}$$

where: $\Delta\nu_h$ – spectral width of the emission homogeneous line, $\Delta\nu_c$ – spectral width of the passive resonator.

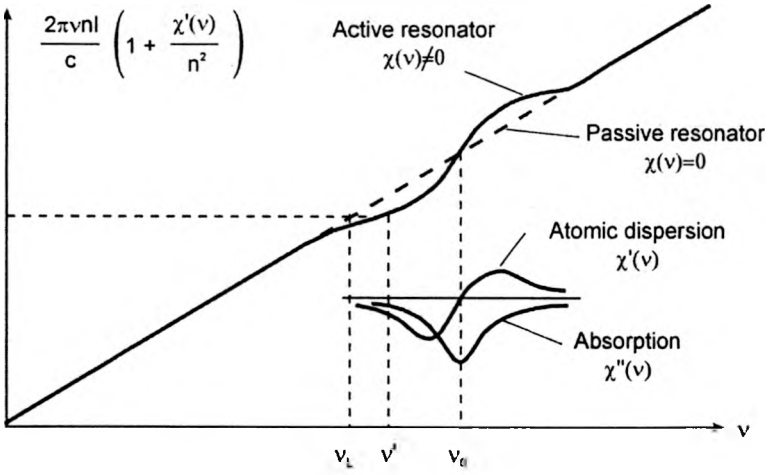

Fig. 28. Pulling effect: ν_0 – centre of the laser gain curve, ν_L – frequency of laser radiation, ν' – pulled frequency, χ, χ', χ'', – refractive index and its components (dispersion and absorption, respectively), n, l – longitudinal mode and resonator length, respectively.

For example, for $\Delta\nu_c = 5$ MHz and the typical CO_2 laser homogeneous gain line $\Delta\nu_h = 100$ MHz, the coefficient of pulling effect near the centre line is equal to $\nu_p = (\nu_0 - \nu_c)/20$, if the frequency is detuned by 20 MHz from the centre we can expect the pulling effect of about 1 MHz.

So, the real stability of the free-running laser is by many orders lower than that described by theoretical limit. To improve frequency stability of the laser, passive and active methods of stabilisation are necessary.

9. Frequency stabilisation of the laser

Frequency fluctuations can be reduced by proper correction of the optical length of the laser resonator. In the first approximation we can tune the frequency of the laser to some characteristic spectral point of the laser line, *i.e.*, to its centre. It is the so-called stabilisation to the centre of the laser gain curve or (from mathematical point of view) so-called extreme stabilisation of the laser frequency.

9.1. Extreme stabilisation of the laser radiation

Figure 29 shows schematically the setup of the frequency stabilisation of the laser. The oscillator modulates one of the laser mirrors TM (perfectly reflecting) with sinusoidal signal. The modulated laser output is detected by a photodetector and

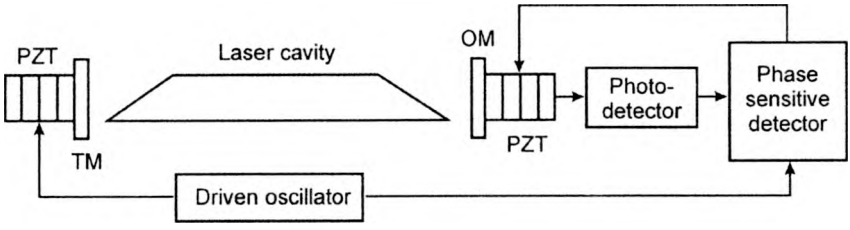

Fig. 29. Setup for the extreme frequency stabilisation of the laser radiation. PZT – piezoceramic transducer, TM, OM – total reflecting and output mirrors, respectively.

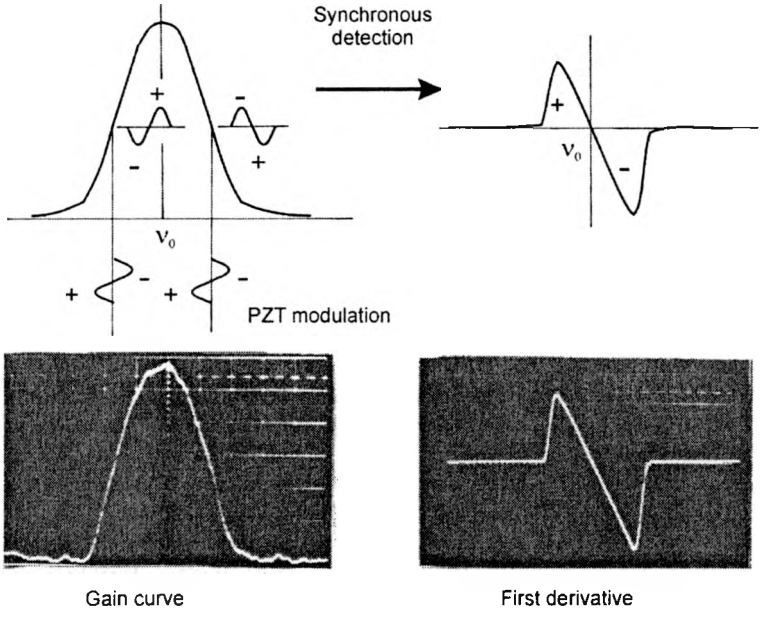

Fig. 30. First derivative method – creation of discrimination signal used in frequency stabilisation servo -loop (experimental signals from [35]).

compared in a phase sensitive detector with the output signal from a driven oscillator. The sign of the output signal from the phase sensitive detector is positive if the modulated laser signal is in phase with the driven oscillator signal, and vice versa. As a result, a discrimination curve of the voltage as an error signal is obtained at the output of the phase detector, and it is used to control the position of one of the laser mirrors (say, OM – output one). In this way, a servo-loop operates close to the 0 – signal on the phase detector or, in other words, close to the centre ν_0 of the laser emission line, see Fig. 30.

Usually the system described improves long-term frequency stability of the order of 10^{-10}. Based on the above method, some more sophisticated stabilisation techniques have been developed, applying narrower spectral features like Lamb dips or inverted Lamb dips in absorption lines of molecules coinciding with the CO_2 spectrum, such as SF_6 or OsO_4 [28], [30], [66].

9.2. Spectral details – saturated absorption method and others

Figure 31 illustrates the methods of laser frequency stabilisation. All of them can be reduced to the extreme stabilisation of the laser frequency. The first derivatives are shown in the figure and the point of stabilisation is indicated. Figure 32 shows experimental data taken from the experiment with a CO_2/SF_6 laser system [35]. The experimental setup contained a CO_2 laser and an external absorption cell filled with a sulphur hexafluoride at the low pressure (the range of mTr). The laser beam passes two times the cell. An incident beam works as a saturated one, and a reflected, week beam works as a detecting one. The setup illustrating the method of saturated absorption frequency stabilisation can be seen in Fig. 33.

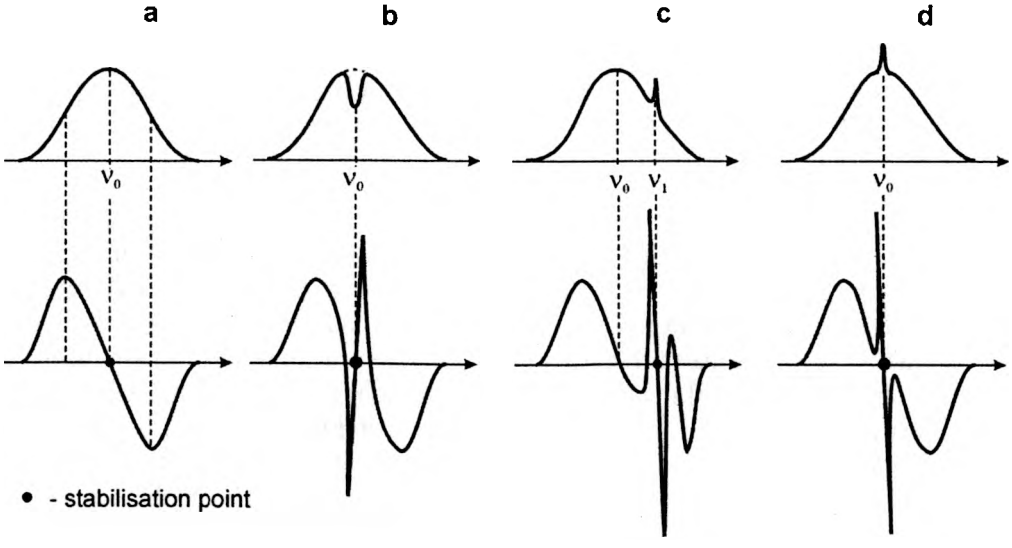

Fig. 31. Laser frequency stabilisation to the center of: **a** – emission line, **b** – Lamb dip, **c** – absorption peak, **d** – absorption peak in the centre of the line.

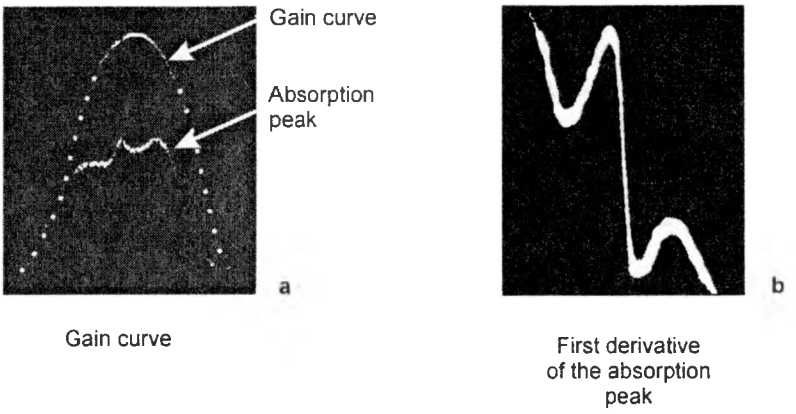

Fig. 32. CO_2 emission line with SF_6 absorption peak (**a**) and first derivative signal of the peak (**b**) – experimental data [35].

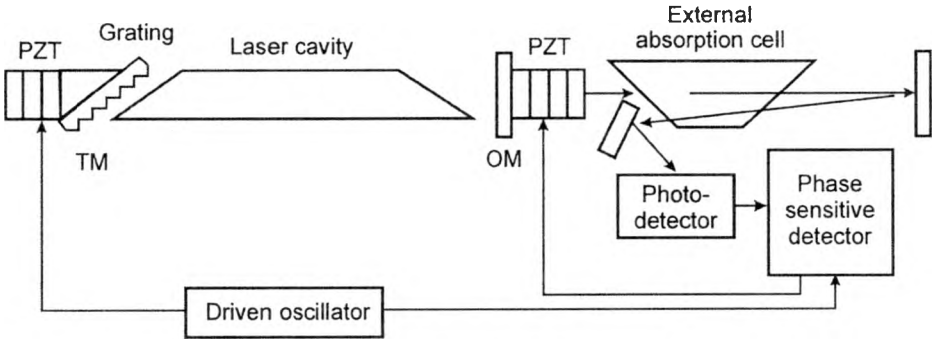

Fig. 33. Saturated absorption method of laser frequency stabilisation (the laser works on a proper emission line selected with a diffraction grating): incident laser beam saturates the absorber in the cell, and a week, reflected beam detects the inverted Lamb dip in the absorber. As a consequence, an absorption peak is observed on the laser output gain curve (see Fig. 32).

As can be seen from Fig. 31, the first derivative of the laser line containing the absorption peak can be quite complicated. The discrimination signal crosses the 0-level (ν-axis) several times. It can disturb the operation of the servo-loop. It is clearly visible in the figure when the position of the peak is outside the centre of the laser line. To avoid this problem, the third derivative of the line profile is used for stabilisation of the laser to the centre of the peak. Figure 34 explains the method. It easy to notice that the second derivative is useless for the extreme stabilisation (the discrimination signal does not cross the 0-level, and it is always negative). As it is seen, the third derivative method allows the background signal to be avoided. The method is used in SF_6/CO_2 [28] or OsO_4/CO_2 [30], [66] laser systems. The absorption spectra of the sulphur hexafluoride and osm tetraoxide are just coincident with some spectral lines of the CO_2 molecule.

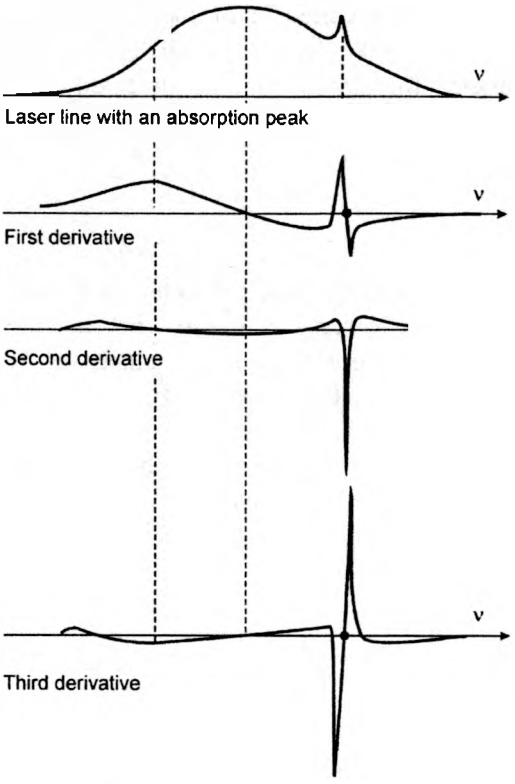

Fig. 34. First, second and third derivatives of the laser emission line with an absorption peak.

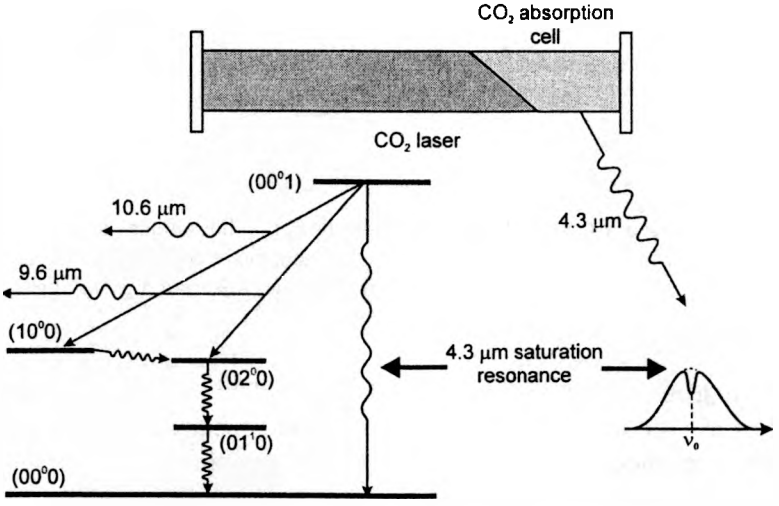

Fig. 35. Extreme stabilisation to the centre of the Lamb dip of the 4.3 μm absorption CO_2 line detected as a sidewall luminescence caused by $0^0 01 - 0^0 00$ transitions in the CO_2 molecule [31].

Stabilisation of the CO_2 laser to the centre of the inverted Lamb dip can be done with the system of the laser coupled with a CO_2 internal absorption cell. The system is presented in Fig. 35. The signal necessary for stabilisation is detected as a luminescence signal from the sidewalls of the laser system and used as a reference signal for the first derivative method of stabilisation [31].

10. Saturated spectroscopy

The setup shown in Fig. 33 can be used as some kind of the spectrograph. It is known that conventional grating spectrographs are not able to resolve "dense" spectra (like absorption spectrum of SF_6 mentioned above). Absorption lines are too close, below Rayleigh criteria. Penetrating the absorbing medium with a laser beam, in such an arrangement as in Fig. 33, the inverted Lamb dip at the centre of each absorption line should occur. As a result, one can observe series of absorption peaks on the profile of the laser line, exactly at the frequencies equal to the frequencies of absorption line centres (see the explanation in Fig. 36). This technique, named saturated spectroscopy,

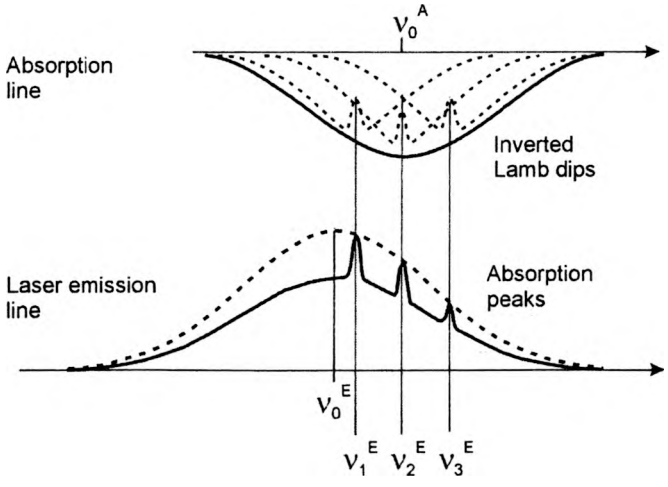

Fig. 36. Saturated absorption spectroscopy method. Resolving of the absorption lines hidden in one line (ν_0^A) observed with a classical spectrograph. Laser beam (with the ν_0^E gain curve centre) saturates the absorber and inverted Lamb dips occurs on the profile of the absorption line. Absorption peaks appear on the profile of the detecting laser beam, ν_1^E, ν_2^E, ν_3^E, respectively, *cf.* Fig. 34.

is commonly used in high resolution spectroscopy. The CO_2 laser is an important element in that kind of a laser spectrograph. The band of the spectrograph can be increased using different methods of the CO_2 laser band spreading, as discussed above [14].

11. Optogalvanic effect

Taking into account the energy balance in the CO_2 laser system, one should remember that the shape of the output laser gain curve depends on laser plasma parameters such as temperature and pressure. On the other hand, the shape of the laser line, or in other words, the laser action, should influence the laser plasma parameters [67]. This effect is very easy to observe in the CO_2 lasers, and it is called optogalvanic effect [68]. Exactness of the representation of the laser output gain curve in optogalvanic signal (or in plasma impedance) is very high [69], [70]. Thus, the effect can be readily used to detectorless stabilisation of the laser radiation, where the changes in plasma impedance (in laser current) are used to generate a frequency-error signal for a frequency servo-loop. Figure 37 shows the oscillograms of the optogalvanic signals detected in CO_2 laser current together with output laser gain curves [69].

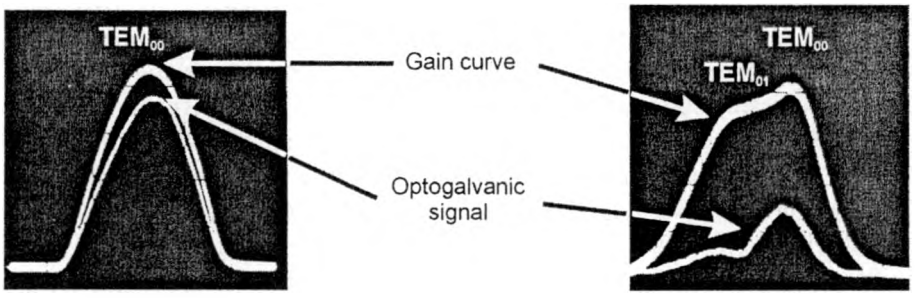

Fig. 37. Optogalvanic signal detected in cw CO_2 laser current for single mode operation (left) and for operation in basic TEM_{00} and transverse TEM_{01} modes (right) [69].

Optogalvanic effect occurs also in RF excited waveguide CO_2 lasers. The optogalvanic signal is detected in RF power reflected by the discharge. The signal is a consequence of variations of the RF plasma impedance of the laser mixture resulting in variable efficiency of power transfer from RF power input to the laser discharge. Here, the phenomenon is called opto-Hertzian effect [71].

12. Conclusions

It has been pointed out in the paper that problems connected with the spectral properties of the CO_2 laser radiation play an important role in some applications of the laser. Many laser measuring techniques are based on spectral properties of the CO_2 laser beam. One of the most sensitive techniques, *i.e.*, heterodyning technique, is widely applied in laser measurements, especially where the intermediate frequencies between known and unknown oscillators are too high for direct measurements. It relies on

another specific spectral feature of the laser, which is high coherence. It is applied in heterodyne spectroscopy and measurements of absolute frequency of the CO_2 hot bands. A simplified, homodyne method is very useful for investigations of the spectral contents of the output laser beam. Both methods can be applied in continuous wave and pulse regimes and they are, as a tool, the most sensitive detector of the spectral contents of the laser output radiation. A very specific feature of the CO_2 laser, *i.e.*, its signature, can be used either to advantage or disadvantage. It can be applied as a diffractive mechanism in laser markers but it can decrease the quality of the output laser beam from waveguide CO_2 laser arrays. The CO_2 laser signature can help in estimating of the changes of the refractive index of the pulse operated laser medium and dynamic behaviour of the pressure and the temperature in the laser cavity, but it can destroy the idea of the diffraction laser marker in pulse regime. The CO_2 laser wavelengths are very suitable for optical pumping of molecular gas media, which involves the development of lasers in a submillimeter region (FIR lasers) – very suitable radiation sources in plasma diagnostics and molecular spectroscopy. Different techniques of the CO_2 laser spectrum spreading are also developed based on spectral properties of the CO_2. They include: the technique of the sequence bands, the technique based on an electronic-to-vibrational energy transfer from an excited Br_2 molecule to a CO_2 molecule, the isotope shift technique. These techniques can spread the CO_2 laser band from 9 to 14 μm. The knowledge about spectral laser fluctuations and their sources is important in designing the frequency stabilised laser devices. More sophisticated stabilisation techniques are based on such spectral phenomena as a Lamb dip (difficult to observe in a CO_2 medium), or inverted Lamb dip. The last technique, for example, stabilisation to the centre of the 4.3 μm saturation resonance, is also based on spectral properties of the CO_2 molecule used as an internal absorber in the laser cavity. Another technique – saturated absorption stabilisation requires a very detailed knowledge about both CO_2 and absorption molecule spectra (like SF_6 or OsO_4) used in the saturated absorption method.

As was mentioned in the introduction, the laser technological devices are usually not sensitive to fine changes of the wavelength of the laser radiation. But some applications of the CO_2 lasers need a good knowledge about their specific, spectral features, which distinguish molecular lasers from much simpler gas atomic lasers. Investigations of the CO_2 laser spectral properties allow us to understand the physics of the laser operation better and makes the proper designing of the laser devices easier.

Acknowledgements – the author is indebted to Prof. Krzysztof M. Abramski for his assistance in this work. This work was supported by the Polish State Committee for Scientific Research (KBN) under grants No. 8 T11B 033 16 and 8 T11B 021 18.

References

[1] RÖSER H. P., Infrared Phys. **32** (1991), 385.
[2] SIEMSEN K. J., WHITFORD B. G., Opt. Commun. **22** (1977) 11.
[3] HILL C. A., JACKSON P. E., IEEE J. Quantum Electron. **24** (1988), 1976.

[4] PLINSKI E. F., WITKOWSKI J. S., ABRAMSKI K. M., Opt. Laser Technol. **32** (2000), 33.
[5] VILLARREAL F., ABRAM R., BLAIR P., *et al.*, Proc. ICALEO'97, Laser Institute of America **83a** (1997), 148.
[6] ABRAMSKI K. M., PLINSKI E. F., WITKOWSKI J. S., NOWICKI R., Conference on Lasers and Electro -Optics Europe, CLEO/Europe'94, Amsterdam, Aug. 28–Sep. 2, 1994, Technical Digest CtuK43, p. 117.
[7] PLINSKI E. F., MAJEWSKI B. W., BEDNARCZYK A. S., ABRAMSKI K. M., *XII Symposium on Gas Flow and Chemical Lasers and High-Power Laser Conference*, GCL/HPL'98, Sankt Petersburg, 1998, Russia, Proc. SPIE **3574** (1998), 500.
[8] HENNIGSEN J. O., IEEE J. Quantum Electron. **13** (1977), 435.
[9] HENNIGSEN J. O., PETERSEN J. C., Infrared Phys. **18** (1978), 475.
[10] REID J., SIEMSEN K., Appl. Phys. Lett. **29** (1976), 250.
[11] REID J., SIEMSEN K., J. Appl. Phys. **48** (1977), 2712.
[12] EVENSON K. M., CHE-CHUNG CHOU, BACH B. W., BACH K. G., IEEE J. Quantum Electron. **30** (1994), 1187.
[13] PETERSEN A. B., WITTIG C., J. Appl. Phys. **47** (1976), 1051.
[14] BETEROV I. M., CHEBOTAYEV V. P., PROVOROV A. S., IEEE J. Quantum Electron. **10** (1974), 245.
[15] GIBSON R. B., BOYER K., JAVAN A., IEEE J. Quantum Electron. **15** (1979), 1224.
[16] FREED CH., IEEE J. Quantum Electron. **18** (1982), 1220.
[17] WENDLAND J. J., BAKER H. J., HALL D. R., Opt. Commun. **154** (1998), 329.
[18] MOCKER H. W., Appl. Phys. Lett. **12** (1968), 20.
[19] COLLEY A. D., ABRAMSKI K. M., BAKER H. J., HALL D. R., IEEE J. Quantum Electron. **27** (1991), 1939.
[20] BORDÉ CH., HENRY L., IEEE J. Quantum Electron. **4** (1968), 874.
[21] KAN T., POWELL H. T., WOLGA G. J., IEEE J. Quantum Electron. **6** (1969), 299.
[22] BORDÉ CH., HENRY L., IEEE J. Quantum Electron. **1** (1970), 81.
[23] KAN T., WOLGA G. J., IEEE J. Quantum Electron. **7** (1971), 141.
[24] RABINOVITZ P., KELLER T., LATOURRETTE J. T., Appl. Phys. Lett. **14** (1969), 376.
[25] FELD M. S., LETOKHOV V. S., Sci. Am. **229** (1973), 69.
[26] BETEROV I. M., CHEBOTAYEV V. P., PROVOROV A. S., Opt. Commun. **7** (1973), 410.
[27] BAZAROV E. N., GERASIMOV G. A., SAZONOV A. I., Kvantovaya Elektron. **8** (1979), 582, (in Russian).
[28] KOMPANEC O. N., KUKUDŽANOV A. R., LETOCHOV V. S., MICHAJLOV E. L., Kvantovaya Elektron. **4** (1973), 28, (in Russian).
[29] VASILENKO L. S., SKVORTSOV M. N., CHEBOTAEV V. P., *et al.*, Opt. Spectrosc. **32** (1972), 609.
[30] BAZAROV E. N., GERASIMOV G. A., GUBIN V. P., POSUDIN JU. I., Izvestija Vuzov SSSR – Radioelektronika **20** (1977), 39, (in Russian).
[31] FREED CH., *Advanced Laser Technology and Applications*, Proc. SPIE **335** (1982), 59.
[32] GOODWIN F. E., NUSSMEIER T. A., IEEE J. Quantum Electron. **4** (1968) 612.
[33] OSHE G. R., HARRIS C. E., ENG R. S., *Advanced Laser Technology and Applications*, Proc.SPIE **335** (1982), 95.
[34] WITTEMAN W. J., *The CO_2 laser*, Springer Series in Optical Sciences, Springer-Verlag, Berlin, New York, 1987.
[35] PLINSKI E. F., Thesis, Wrocław University of Technology, Institute Telecommunications and Acoustics, internal Report, Wrocław, 1983.
[36] PLINSKI E. F., WITKOWSKI J. S., Unpublicated data, Wrocław University of Technology, 1999.
[37] SUTTER L. V., Opt. Eng. **20** (1981), 769.
[38] PLINSKI E. F., BĄCZYK K., ABRAMSKI K. M., *et al.*, *Laser Technology V: Physics and Research and Development Trends*, Sept. 23–27, 1996, Szczecin–Świnoujście, Poland, Proc. SPIE **3186** (1996), 275.
[39] WAKSBERG A. L., BOAG J. C., SIZGORIS S., IEEE J. Quantum Electron. **7** (1971), 29.
[40] SCHIFFNER G., IEEE J. Quantum Electron. **8** (1972), 877.
[41] BUHOLZ N. E., IEEE J. Quantum Electron. **18** (1982), 1326.

[42] NATH A. K., CHATTERJEE U. K., IEEE J. Quantum Electron. **16** (1980), 1263.
[43] PLINSKI E. F., WITKOWSKI J. S., Opt. Commun. **176** (2000), 207.
[44] PLINSKI E. F., WITKOWSKI J. S., ABRAMSKI K. M., *XI International Symposium on Gas Flow and Chemical Lasers and High-Power Laser Conference*, GCL/HPL'96, Edinburgh, 1996, Scotland, Proc. SPIE **3092** (1996), 206.
[45] MAJEWSKI B., Diploma work, supervisor E. F. Plinski, Wrocław University of Technology, Institute Telecommunications and Acoustics, internal Report, Wrocław, 1996.
[46] ABRAMSKI K. M., COLLEY A. D., BAKER H. J., HALL D. R., IEEE J. Quantum Electron. **32** (1996), 340.
[47] CLARKSON W. A., HANNA D. C., Opt. Lett. **21** (1996), 375.
[48] ABRAMSKI K. M., PLIŃSKI E. F., WITKOWSKI J. S., *Conference on Lasers and Electro-Optics Europe*, CLEO/Europe'94, Amsterdam, *Technical Digest*, 1994; paper CTuK43: 117
[49] LACHAMBRE J.-L., MACFARLANE J., OTIS G., LAVIGNE P., Appl. Phys. Lett. **32** (1978), 652.
[50] CHRISTENSEN C. P., POWELL P. X., DJEU N., IEEE J. Quantum Electron. **9** (1980), 949.
[51] PLINSKI E. F., BEDNARCZYK A. S., MAJEWSKI B. W., ABRAMSKI K. M., *11-th Slovak-Czech-Polish Optical Conference on Wave and Quantum Aspects of Contemporary Optics*, Stara Lesna, Slovakia, Proc. SPIE **3820** (1998), 286.
[52] YAMANAKA M., Rev. Laser Eng. **3** (1976), 253.
[53] CHANG T. Y., BRIDGES T. J., Opt. Commun. **1** (1970), 423.
[54] BOBROVSKIJ A. N., VEDENOV A. A., KOŻEVNIKOV A. W., SOBOLENKO D. N., Pisma Zh. Eksp. Teor. Fiz. **29** (1979), 589, (in Russian).
[55] FETTERMAN H. R., SCHOSSBERG H. R., WALDMAN J., Laser Focus Word **8** (1972), 42
[56] KOEPF G. A., Infrared Phys. **18** (1978), 469.
[57] TOBIN M. S., JENSEN R. E., IEEE J. Quantum Electron. **13** (1977), 481.
[58] ABRAMS R. L., PINNOW D. A., J. Appl. Phys. **41** (1970), 2765.
[59] BUHRER C. F., BAIRD D., CONWELL E. M., Appl. Phys. Lett. **1** (1962), 46.
[60] LUND M., COGAN J. N., DAVIS J. A., Rev.Sci. Instrum. **50** (1979) 791.
[61] ABRAMS R. L., Appl. Phys. Lett. **25** (1974), 304.
[62] LEEB W. R., Appl. Opt. **14** (1975), 1706.
[63] EVENSON K. M., JENNINGS D. A., PETERSEN R. F., *et al.*, IEEE J. Quantum Electron. **13** (1977), 442.
[64] MANITA O. F., Prib.Techn.Eksp. **2** (1979), 240, (in Russian).
[65] SCHAWLOW A. L., TOWNES C. H., Phys. Rev. **112** (1958), 1940-1949.
[66] DOMNIN JU. S., KOTELAJEVSKIJ N. B., TATARENKOV V. M., *et al.*, Pisma Zh. Eksp. Teor. Fiz. **30** (1979), 269 (in Russian).
[67] SKOLNICK M. L., IEEE J. Quantum Electron. **6** (1969) 139.
[68] SMITH A. L. S., MOFFAT S., Opt. Commun. **30** (1979), 213.
[69] PLINSKI E. F., ABRAMSKI K. M., Opt. Commun. **50** (1984), 162.
[70] NOWICKI R, PLINSKI E. F., RZEPKA J., Opt. Commun. **53** (1985), 113.
[71] JACKSON P. E., ABRAMSKI K. M., HALL D. R., Appl. Phys. B **47** (1988), 149.

Received April 4, 2000